Bulgarian Chemical Communications, Volume 55, Special Issue C (pp. 75–79) 2023 *DOI: 10.34049/bcc.55.C.0008*

Personalized approach in defining the level of interest during lung electrical impedance tomography

I. Minev[1,2*], V. Jukic[3], T. Gogova[2], N. Traykova[1,2]

[1] *Department of Anesthesiology, Emergency, and Intensive care medicine; Medical University of Plovdiv, Bulgaria 15A, Vasil Aprilov, Blvd., Plovdiv 4000*
[2] *University Hospital "St. George", Plovdiv, Bulgaria*
[3] *ServerNet Srl., Trieste, Italy*

Received: November 2023; Revised: December 2023

Electrical impedance tomography (EIT) is a non-invasive method for personalized monitoring of lung ventilation at the bedside. Although for years in clinical practice there are no clear recommendations for optimal placement of the electrodes. The objective is to develop a protocol for defining the level of interest, electrode belt positioning and individualized reconstruction of the EIT images. A computed tomography (CT) scan analysis is used for defining the level of interest and providing reference points for belt positioning. The margins of the patient's thorax are determined by applying a fem mesh to the CT image. Subsequently the raw data from the EIT is reconstructed within the individualized contour of the thorax reflecting the body structure of the patient. Applying the protocol for defining a level of interest, belt positioning and individualized reconstruction of the EIT images resulted in significant conformity between the lung areas on the CT image and the reconstructed EIT image taken at the corresponding thoracic level. Thus, the limitations for placing the EIT belt at different, than initially recommended positions are surmounted and indications for potential clinical application of EIT in conditions which are characterized by heterogeneously disseminated or solitary lesions. The personalized approach in EIT application reveals its potential to support the optimization of mechanical ventilation according to the individual condition and disease, especially in case of heterogeneously disseminated or solitary lesions.

Keywords: EIT, electrode belt positioning, personalized monitoring, mechanical ventilation.

INTRODUCTION

Electrical impedance tomography (EIT) is designed and promoted as a noninvasive method [1] for personalized monitoring [2, 3] of lung ventilation at the bedside. The EIT devices are significantly informative [4] about the heterogeneous characteristics [5] of lung function, caused by different pathological conditions [6–9]. Although four decades in clinical practice [10], its potential is not fully revealed. The informational value of the method is significantly reduced [11] due to the fact that there are no guidelines for sufficient personalization of the acquired data. There are several reasons that limit EIT application in the intensive care units, narrowing its use. The first is the lack of clear recommendations for optimal placement [12] of the EIT electrodes. It is caused by the absence of instructions on determining the level of interest. Thus, there is no possibility to correct the data of the raw EIT images in accordance with the patient's anatomic characteristics and create reliable images with high resolution. Nevertheless, the application of the EIT at certain levels [13] of the thorax restricts its ability to assess the pathological process development if it is located elsewhere. Therefore, our goal is to develop a protocol for defining the level of interest, electrode belt positioning and individualized reconstruction of the EIT images.

MATERIALS AND METHODS

A retrospective analysis of anonymized raw data from the EIT monitor (Swisstom BB2 EIT Monitor) in comparison with thoracic CT scans (Siemens

* To whom all correspondence should be sent:
E-mail: ivaylo.minev@mu-plovdiv.bg

Somatom Definition AS) was performed. There was used data of patients with lung contusion, admitted in the ICU of the Department of Anesthesiology and Intensive care, University hospital "St. George" – Plovdiv, Bulgaria. Based on analysis of thoracic CT scans the level of interest was defined as the most significant intersection between the injured lung zones and the plane where the electrodes for EIT should be placed. According to the study protocol a radiologist proposed appropriate anatomical markers on the patient's skin. These reference points were used to guide the placement of the belt with EIT electrodes. A two-dimensional fem mesh was created. The spatial determination of the thoracic borders was made by placing the fem mesh onto the CT scan image taken at the level of interest and adjusting the mesh to the contour of the patient's thorax. The raw EIT data was processed within this personalized contour, followed by a reconstruction of the raw EIT image, reflecting patient anatomical characteristics.

RESULTS AND DISCUSSION

Some pathological processes cause heterogeneous lung tissue [14] alteration, which does not correspond to the recommended levels [12] for positioning of the EIT belt thus compromising the conclusions [15] of the EIT results. The areas affected by these conditions could be identified by more comprehensive image diagnostic methods like CT and MRI. We provide researchers with methodology for reasonable definition of unconventional levels of interest determined by the location of the lesion and how to define the EIT belt positioning. In our protocol we have chosen the CT image as a reference method.

Process description

Based on the CT scan analysis we define the level of interest (topographically described with skin markers and angle) as the slice containing the largest area of the investigated pathological process (Fig. 1).

This determines the level of the EIT belt positioning. Such positioning ensures that the raw EIT image will contain the required information for description of the injured zones.

According to the study protocol a radiologist proposed appropriate anatomical markers on the patient's skin. These reference points were used to guide the placement of the belt with EIT electrodes (Fig. 2).

The initial EIT image by default has a circular shape (Fig. 3) that does not correspond to the contour of the patient's thorax. Therefore, the primary signal in every pixel of the raw image will not correctly represent the impedance values generated in the patient thorax.

To overcome this discrepancy, the initial image should be reshaped in order to match the real contour of the patient thorax. To support the EIT image reconstruction optimization, we provide a rationale on how to use a fem mesh for precise matching of the intersection of the patient thorax obtained by CT with the EIT image and increase the informational

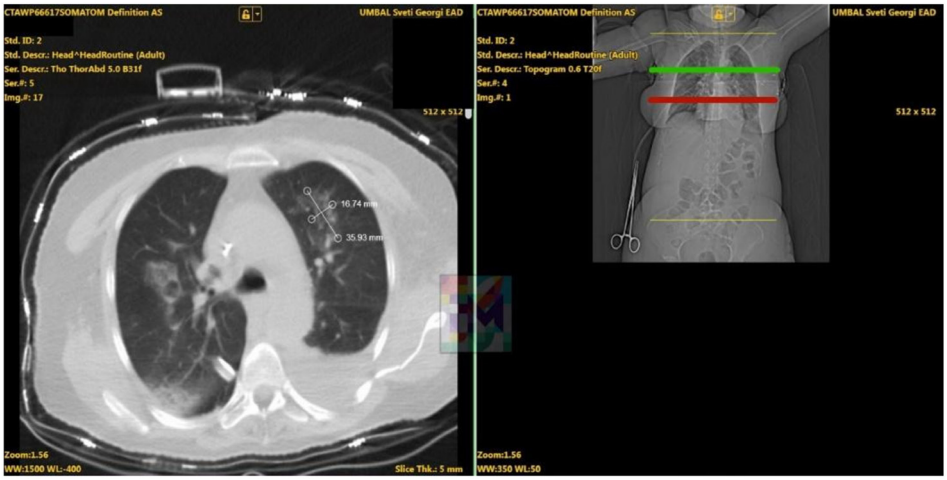

Fig. 1. A CT scan of a patient with chest trauma.

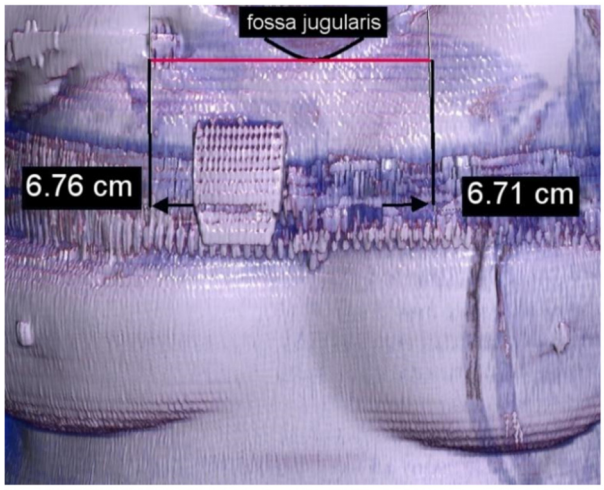

Fig. 2. CT reconstruction of the body with distance to the skin markers.

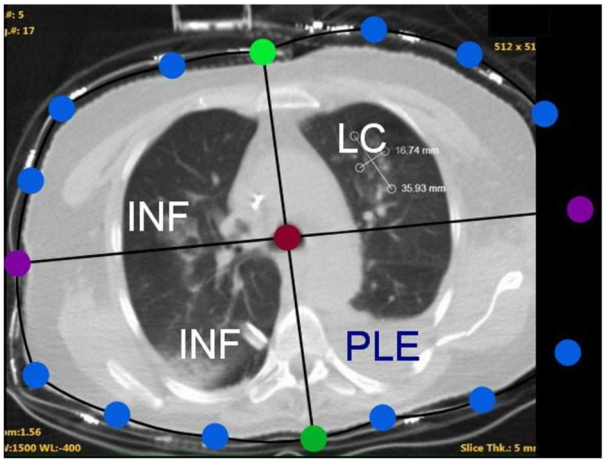

Fig. 4. The fem-mesh over imposing on to the CT scan.

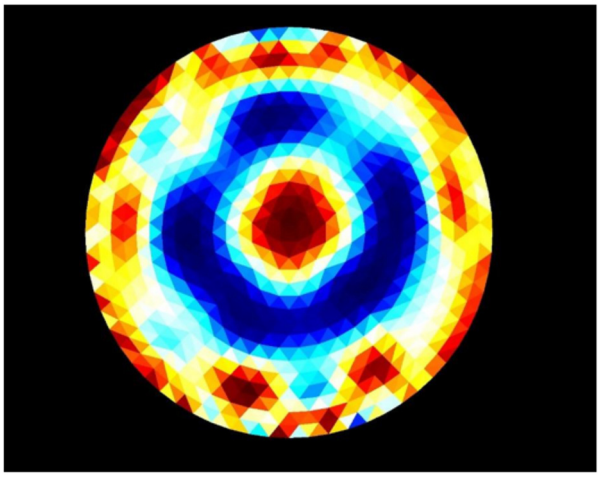

Fig. 3. Initial non-personalized EIT image.

value of the functional EIT images taken at unconventional levels of interest.

We created a two-dimensional fem mesh of 16 cartesian points - 4 pivotal points defining the anteroposterior and transverse diameters of the patient's thorax, one constrained center, 3 points on each quadrant (Fig. 4).

There are some constraints. The points of the mesh could not be too close or too distant or overlap the rule of the mesh, the topology could not be folded, because it will create null value [16]. The CT scan image is used for measuring 4 points defining antero-posterior and transverse diameters of the thorax. Following that a reference image of the CT scan at the level of interest (angle, points) is generated. The reference image size must be at least 512×512 pixels with resolution of minimum 20 pixels per cm^2. Placing the points of the mesh on the contour of the patient's thorax (Fig. 4) on the reference image results in spatial definition of the thoracic borders.

The primary use of the mesh is to calculate data. We start with normalized condition and create a reconstruction of the image. We do the image reconstruction with a fem model of more than 20000 elements which describes a standard thorax with a resolution better than around 5×5 mm.

Following algorithm optimization and fine tuning, higher resolution of the EIT image is achieved. After the EIT scan is obtained the raw file of numerical data from the EIT device is imported into the fem model and a new personalized static EIT image is generated. The data is processed by input filter – the voltage is being calculated out of current and impedance pairs and oversaturated and poorly saturated leads are taken out. The result is 32×32(1024) voltage measurement used by inverse solver [17] to create the static image on the fem model created by a specific mesh matching the CT image.

The result is a color-coded two-dimensional fem diagram representing the body composition of the patient in that specific slice. It contains no patient identification or protected data information. This personalized static EIT image should "perfectly" fit over an imposed CT scan taken at the same level of interest. The degree of match between the EIT static image and the CT scan is assessed by calculating the % of overlapping conformity.

Protocol application

On Figure 1 a thoracic CT scan of a patient with lung contusion is presented. The level and the angle of positioning of the electrodes is defined by the plane with the largest intersection with the injured zones (the lung contusion – LC, the infiltrative changes – INF and the pleural effusion – PLE). This level (indicated in green) is significantly higher than the recommended by the vendor V intercostal space (indicated in red). Therefore, in patients with lung contusion at a level different than the recommended level of belt positioning, following the vendor's instructions would not result in reliable information about the distribution of lung ventilation in the injured zones.

Figure 3 displays a non-personalized EIT image of the same patient. By definition it is constructed within the contour of a circle. The resolution is low and the correspondence to the real patient's thorax anatomy is weak. Furthermore, the initial reconstruction is made according to a shape of a thorax transection at level of fifth-sixth intercostal space of an ideal patient and a blend covering the thoracic wall and mediastinum is used (Fig. 5).

The application of the protocol for defining the level of interest, electrode belt positioning and individualized reconstruction of the EIT images, resulted in significant conformity between the CT scan and the EIT image taken at the same thoracic level (Fig. 6).

The impedance was not equally distributed. Several abnormality zones were marked and compared with the corresponding zones of the CT image. The

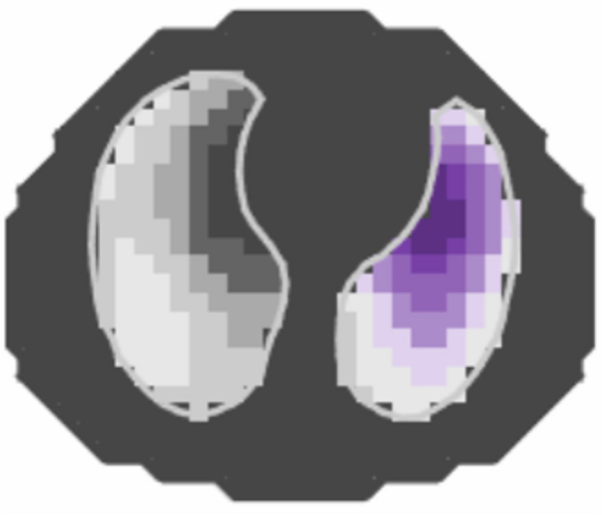

Fig. 5. EIT image with over-imposed blend.

visual analysis revealed considerable sensitivity of the EIT to gas and water distribution [18, 19].

Dorsally and bilaterally on the EIT image an impedance abnormality with horizontal ventral border was observed. On both sides of the CT scan signs related to water accumulation were visible. On the left there was pleural effusion – PLE and on the right infiltrative process – INF. It is important to point out that the ventral margin of the pleural effusion on the CT scan matched the change in the impedance distribution on the EIT image. In contrast, the ventral margin of the infiltrative process was lower than the corresponding change in the impedance, suggesting that the electrical impedance tomography provides higher

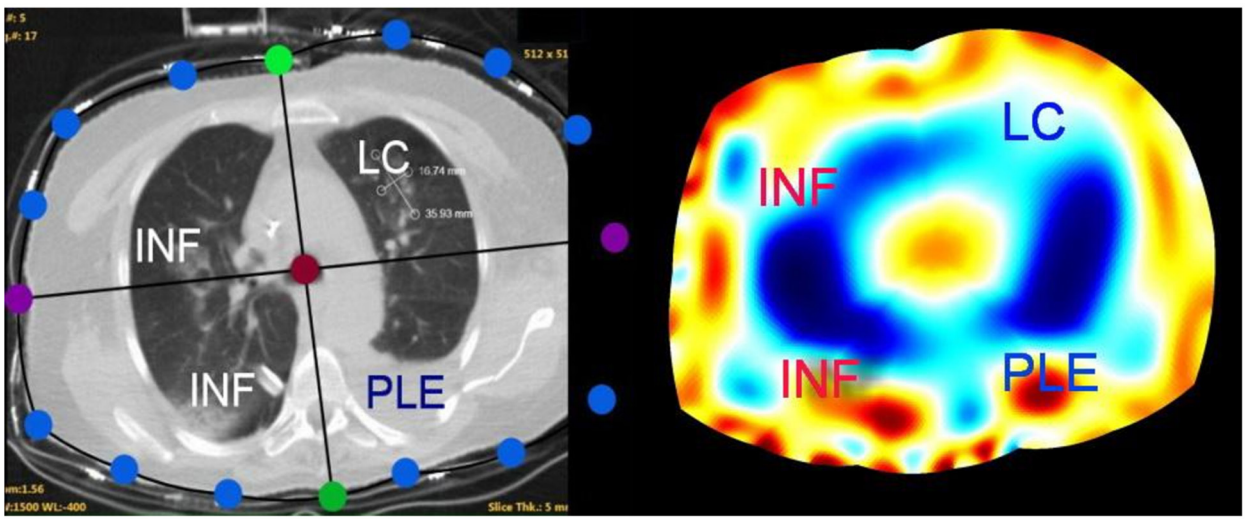

Fig. 6. The personalized EIT static image in comparison to the CT scan.

sensitivity to the changes in water distribution than the CT scan but lower resolution. EIT abnormalities reflect the tissue function alteration and visualize prospective changes prior organizational structural changes [20]. Different factors affect the water accumulation and the impedance changes in these two pathological focuses. Pleural effusions are poor of biological membranes in the liquid [21–23] and gravity is a major factor. The infiltration is related to inflammation that results in water accumulation in the lung tissue due to changes in biological membrane permeability and is dependent on gravity and lung tissue architecture (vascularization and ventilation in the segments). In these regions restricted distribution of ventilation [24, 25] is observed on dynamic images. Considering the differences in the pathophysiology further investigation should be performed.

CONCLUSIONS

The protocol for defining the level of interest, electrode belt positioning and individualized reconstruction of the EIT images overcomes the limitations for placement of the electrode belt at levels different than the initially recommended. In addition, it improves EIT clinical application for optimization of lung ventilation monitoring. Furthermore, the protocol reveals the potential of the EIT to be used for monitoring the dynamics of the lung injury in conditions, characterized by heterogeneous dissemination or solitary lesions.

Acknowledgments: *Project BG05M2OP001-1. 002-0005 – Competence Center "Personalized Innovative Medicine (PERIMED)", financed by Operational Program "Science and Education for Smart Growth", EU, ESIF; Project NO-08/2021 "Investigating the capabilities of EIT as a clinical method for monitoring lung injury dynamics in patients with thoracic trauma", MU-Plovdiv.*

REFERENCES

1. S. Leonhardt, B. Lachmann, *Intensive Care Med*., **38**, 1917 (2012).
2. T. Muders, H. Luepschen, C. Putensen, *Curr. Opin. Crit. Care*, **16**, 269 (2010).
3. J. M. Constantin, S. Perbet, J. Delmas, E. Futier, *Crit. Care*, **18**, 164 (2014).
4. B. Vogt, S. Pulletz, G. Elke, Z. Zhao, P. Zabel, N. Weiler, I. Frerichs, *J. Appl. Physiol.*, **113**, 1154 (2012).
5. R. Bhatia, G. M. Schmölzer, P. G. Davis, D. Tingay, *Intensive Care Med*., **38**, 308 (2012).
6. S. Pulletz, M. Kott, G. Elke, D. Schädler, B. Vogt, N. Weiler, I. Frerichs, *Multidiscip. Respir. Med*., **7**, 44 (2012).
7. B. Vogt, Z. Zhao, P. Zabel, N. Weiler, I. Frerichs, *Am. J. Physiol. Lung Cell. Mol. Physiol.*, **311**, L8 (2016).
8. R. E. Serrano, L. B. de, O. Casas, T. Feixas, N. Calaf, V. Camacho, I. Carrió, P. Casan, *J. Sanchis, P. Riu, Physiol. Meas*., **23**, 211 (2002).
9. Z. Zhao, U. Müller-Lisse, I. Frerichs, R. Fischer, K. Möller, *Physiol. Meas*., **34**, N107 (2013).
10. A. Adler, D. Holder, Electrical Impedance Tomography: Methods, History and Applications, ISBN: 978-0-429-39988-6, DOI: 10.1201/9780429 399886, 2022.
11. W. R. Lionheart, *Physiol. Meas*., **25**, 125 (2004).
12. J. Karsten, T. Stueber, N. Voigt, E. Teschner, H. Heinze, *Crit. Care*, **20**, 3 (2016).
13. S. Krueger-Ziolek, B. Schullcke, J. Kretschmer, U. Müller-Lisse, K. Möller, Z. Zhao, *Physiol. Meas*., **36**, 1109 (2015).
14. J. Gao, S. Yue, J. Chen, H. Wang, *Bio-Med. Mater. Eng*., **24**, 2229 (2014).
15. F. Reifferscheid, G. Elke, S. Pulletz, B. Gawelczyk, I. Lautenschläger, M. Steinfath, N. Weiler, I. Frerichs, *Respirology*, **16**, 523 (2011).
16. J. T. Schwartz, Differential Geometry and Topology, G&B Science Pub, ISBN-13: 978-9990196689, 1968.
17. H. Wang, E. Zimmermann, M. Weigand, H. Vereecken, J. A. Huisman, Geophys. *J. Int.*, **235**, 2888 (2023).
18. C. Trepte, C. Phillips, J. Solà, A. Adler, S. Haas, M. Rapin, S. Böhm, D. Reuter, *Crit. Care*, **20**, 18 (2016).
19. F. Fu, B. Li, M. Dai, S. J. Hu, X. Li, C. H. Xu, B. Wang, B. Yang, M. X. Tang, X. Z. Dong, Z. Fei, X. T. Shi, *PLoS One*, **9**(12), e113202 (2014).
20. S. Hannan, M. Faulkner, K. Aristovich, J. Avery, M. Walker, D. Holder. *NeuroImage*, **209**, 116525 (2020).
21. J. M. Porcel, M. Azzopardi, C. F. Koegelenberg, F. Maldonado, N. M. Rahman, Y. C. Lee, *Expert Rev. Respir. Med*., **9**, 801 (2015).
22. S. P. Chubb, R. A. Williams, *Clin. Biochem. Rev*., **39**(2), 39 (2018).
23. P. Kunst, A. Vonk Noordegraaf, E. Raaijmakers, J. Bakker, A. Groeneveld, P. Postmus, P. de Vries, *Chest*, **116**, 1695 (1999).
24. J. Spaeth, K. Daume, U. Goebel, S. Wirth, S. Schumann, *Br. J. Anaesth*., **116**, 838 (2016).
25. T. Becher, B. Vogt, M. Kott, D. Schädler, N. Weiler, I. Frerichs, *PLoS One*, 11, e0152267 (2016).